



SUBJECT AREAS:
CLIMATE CHANGE
PALAEOCLIMATE
BIOGEOCHEMISTRY
EARTH SCIENCES

Received
2 May 2012

Accepted
14 August 2012

Published
29 August 2012

Correspondence and
requests for materials
should be addressed to
L.v.G. (Lucien.
vongunten@giub.
unibe.ch)

Proxy-to-proxy calibration: Increasing the temporal resolution of quantitative climate reconstructions

Lucien von Gunten^{1,2,3}, William J. D'Andrea⁴, Raymond S. Bradley¹ & Yongsong Huang⁵

¹Climate System Research Center, University of Massachusetts, Amherst, USA, ²Geological Institute, ETH, Zürich, Switzerland, ³Institute of Geography and Oeschger Center for Climate Change Research, University of Bern, Switzerland, ⁴Lamont-Doherty Earth Observatory of Columbia University, Palisades, NY, USA, ⁵Department of Geological Sciences, Brown University, Providence, RI, USA.

High-resolution paleoclimate reconstructions are often restricted by the difficulties of sampling geologic archives in great detail and the analytical costs of processing large numbers of samples. Using sediments from Lake Braya Sø, Greenland, we introduce a new method that provides a quantitative high-resolution paleoclimate record by combining measurements of the alkenone unsaturation index (U_{37}^K) with non-destructive scanning reflectance spectroscopic measurements in the visible range (VIS-RS). The proxy-to-proxy (PTP) method exploits two distinct calibrations: the *in situ* calibration of U_{37}^K to lake water temperature and the calibration of scanning VIS-RS data to down core U_{37}^K data. Using this approach, we produced a quantitative temperature record that is longer and has 5 times higher sampling resolution than the original U_{37}^K time series, thereby allowing detection of temperature variability in frequency bands characteristic of the AMO over the past 7,000 years.

The Arctic exerts a large influence on global climate and is currently undergoing profound environmental changes^{1–3}. In order to put these into a larger context, and to anticipate future climate and environmental changes, we must understand the degree to which, and the reasons why, Arctic temperatures have varied in the past. There are limited options for paleotemperature reconstruction in the Arctic region. Tree ring-based records are generally shorter than a millennium and low-frequency (multi-decadal to centennial) changes in temperature are probably not fully captured by such reconstructions^{4,5}. Ice cores are geographically restricted (high latitudes and altitudes), and provide temperature estimates atop ice sheets, which can differ significantly from temperatures at sea level⁶. Lake sediments are excellent archives of Arctic temperature because they comprise various materials that can be used for paleoenvironmental reconstruction and, as a dominant feature of the Arctic landscape, provide the potential for a dense network of paleoclimate reconstructions. Lake-based reconstructions are contingent upon observed relationships between the sedimentary component of interest and one or more environmental or climatic variable, and quantitative records require calibration.

Here we introduce “proxy-to-proxy” (PTP) calibration, using visible range scanning reflectance spectroscopic (VIS-RS) data, obtained through rapid, non-destructive, and inexpensive analysis of sediment cores at very high resolution^{7,8}. We report a PTP calibration between the VIS-RS RABD_{660:670} index⁷ and alkenone unsaturation (U_{37}^K) data^{9,10}, from two overlapping cores from lake Braya Sø, west Greenland. U_{37}^K was calibrated *in situ* in Braya Sø during two field seasons and a 5,600 year long U_{37}^K record from Braya Sø sediments was replicated in a second lake in the region⁹. This and additional work^{11–13} provide strong evidence that U_{37}^K reflects past lake water temperature. The index RABD_{660:670}⁷ represents chlorin (molecules deriving from chlorophyll, primarily from autochthonous primary productivity) content within the sediment and therefore the balance between autochthonous primary productivity in the photic zone and organic matter preservation in lake sediments. Braya Sø is currently a meromictic lake with permanently anoxic bottom waters. The preservation of fine (< 1 mm), uninterrupted laminations in the sediments indicates that the lake bottom has been suboxic to anoxic during the past 7,000 years. Therefore, preservation potential is unlikely to have varied substantially and we interpret RABD_{660:670} of Braya Sø sediments as a record of autochthonous primary productivity.

Autochthonous productivity in arctic lakes is positively correlated with summer temperature^{14–18} through the impact of temperature on 1) the duration of the ice-free period (i.e., the productive season) and, potentially, 2) the

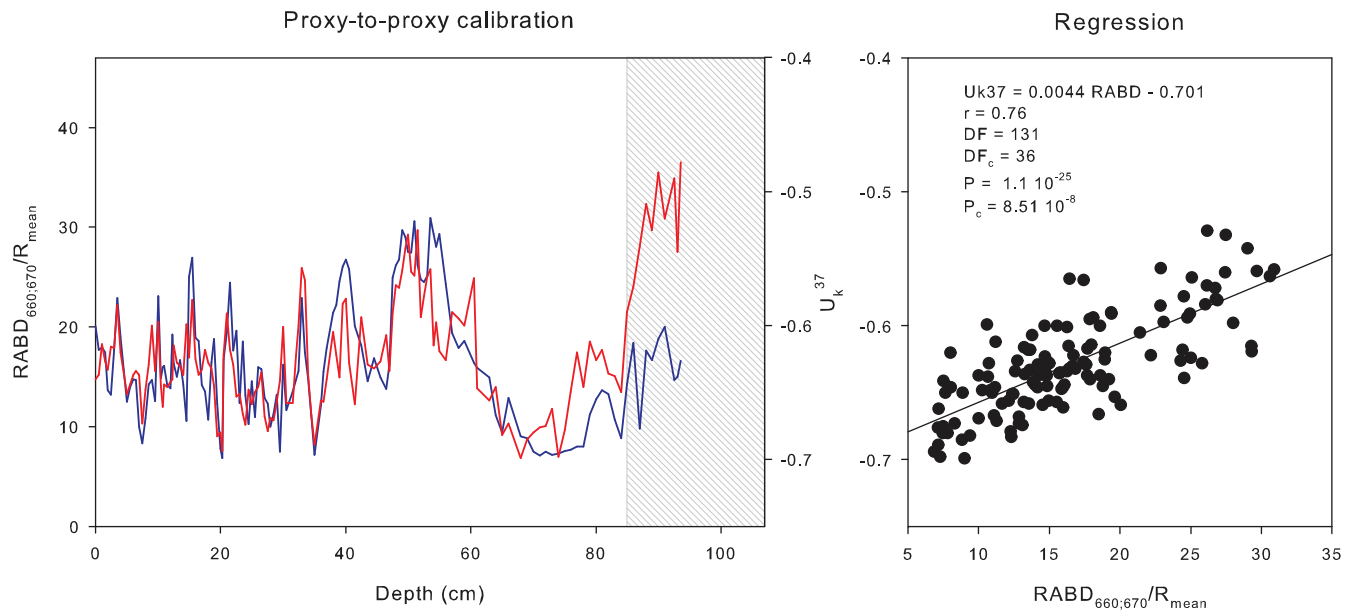


Figure 1 | Proxy-to-proxy calibration. **Left panel:** Proxy-to-proxy calibration between the resampled VIS-RS RABD_{660,670} (blue) and alkenone U_{37}^K data (red). The data below 84 cm were not used for the calibration (shaded area). **Right panel:** The regression plot and calibration statistics. DF: degrees of freedom, P: P-Value. The subscript “c” denotes values corrected for autocorrelation and trends.

nutrient flux to lakes from the watershed¹⁹. It follows that the chlorin content in Braya Sø sediments (quantified with RABD_{660,670}) would be closely related to summer temperature.

Results

Developing the proxy-to-proxy calibration. Because the RABD_{660,670} data were obtained at much higher resolution than the U_{37}^K data, for calibration purposes we numerically re-sampled them to match the sampling interval of the U_{37}^K data from 0–84 cm in the core (Fig. 1). Both the timing and the amplitude of variability are very similar for both measurements, with the only notable discrepancies occurring between 54–61 and 69–84 cm. The Pearson’s r of 0.76 for the regression between the RABD_{660,670} and U_{37}^K data is highly significant ($P_c = 8.51 \cdot 10^{-8}$). The RMSEP (root mean square error of prediction) for both the Ordinary Least Squares (OLS) and Standard Major Axis (SMA) regression methods was small (OLS: 0.0243 and SMA: 0.0264 U_{37}^K units) and the verification statistics high (OLS: RE = 0.62, CoE = 0.55; SMA: RE = 0.58, CoE = 0.50). Both the OLS and SMA models yield very similar results (with SMA producing only slightly larger amplitudes of variation) implying that the model choice is not critical in this case. The U_{37}^K measurements below 84 cm were not

used for the calibration because they reach anomalously high values (shaded area in Fig. 1). These high values correspond to the first appearance of alkenones in Braya Sø and, unlike the rest of the U_{37}^K record, cannot be validated with results from a nearby lake⁹. The new chlorin based reconstruction strongly supports the temperature record presented in D’Andrea et al. (2011)⁹, and demonstrates that Lake Braya Sø is well suited to reconstruct past temperatures.

Improvements over original data series. When the calibration equation between RABD_{660,670} and U_{37}^K is applied to the full RABD_{660,670} data set, sampling resolution of the U_{37}^K -based temperature record is improved five-fold (661 instead of 131 measurements) (Fig. 2). Due to the additional uncertainty introduced by the PTP calibration, the RMSEP is larger (OLS: 1.66°C and SMA: 1.71°C) than for the U_{37}^K reconstruction alone (1.33°C). We note that our reported RMSEP is an overestimate because it does not take into account the cross-validation of the two temperature proxies provided by the PTP approach; however, further work is needed to develop a statistical quantification of this impact.

Spectral analysis performed on the higher-resolution (PTP-based) OLS temperature reconstruction allows detection of multi-decadal variability that occurred over shorter timescales than are detectable by spectral analysis of the original U_{37}^K -based temperature reconstruction of D’Andrea et al. (2011)⁹ (Fig. 3). The U_{37}^K reconstruction exhibited two prominent frequency peaks at 230 and 297 years but those were not significant at the critical false-alarm level identified at 98% (see Methods). In contrast, the PTP reconstruction had frequency peaks exceeding the 99.7% false alarm level at 24–25, 63–64 and 81–82 years. The latter two correspond to the periodicities of 63–64 and ~81 years associated with the Atlantic Multidecadal Oscillation (AMO)^{20–22}.

Comparison with an independent AMO record. Figure 4 shows that our record shares a significant common spectral signal in the range of 51–64 years with the tree ring-based sea surface temperature (SST) reconstruction of Gray et al. (2004)²³ which was used to reconstruct changes in the AMO since 1567 CE. When both records are band-pass filtered in the 50–70 year range to isolate the AMO signal, the reconstructed variance in both reconstructions is very similar (Fig. 5). We therefore suggest that our record provides

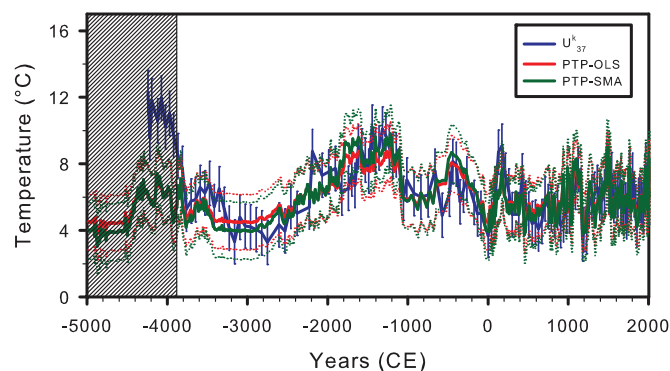


Figure 2 | PTP-derived temperature reconstructions. Ordinary least squares regression (OLS) in red; Standard Major Axis regression (SMA) in green. The dashed lines show the respective RMSEP. The alkenone-based (U_{37}^K) reconstruction and its RMSEP (vertical lines) in blue.

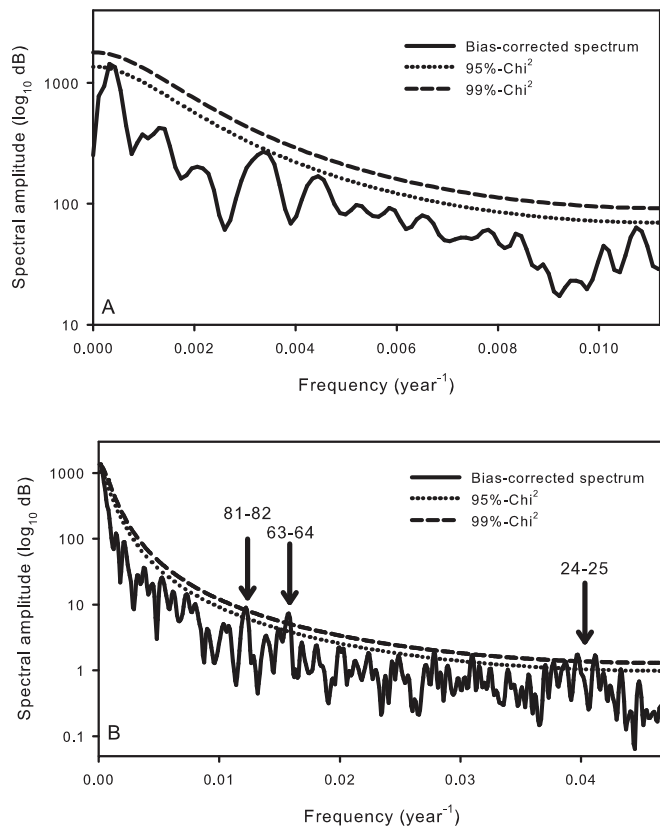


Figure 3 | Spectral analysis of time-series. Bias-corrected spectra of (A) the original U_{37}^K temperature reconstruction and (B) the new PTP temperature reconstruction. Solid line is the spectrum, dashed line is the 99% and dotted line is the 95% false-alarm level. Frequencies are reported as 1/years and spectral amplitudes are plotted on a logarithmic decibel [dB] scale.

insight into the long-term behavior of the AMO. A cross spectral analysis of the band-pass filtered records shows that the Gray et al. (2004)²³ leads our new AMO series by ca. 20 years. Although there could be a mechanistic explanation for this phase shift, a systematic offset due to dating uncertainties cannot be excluded, and indeed, this may be the more likely explanation. The full 7,000 year long

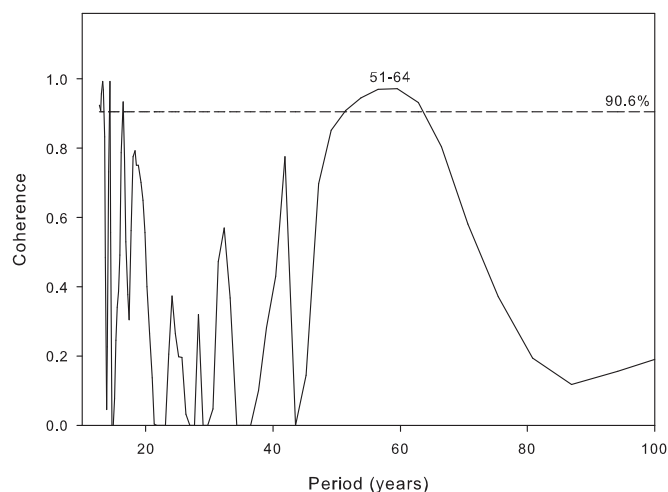


Figure 4 | Cross-spectral analysis with SST reconstruction. Blackman-Harris 3-Term Cross-spectral coherence plot of the PTP (this study) and the Gray et al. (2004)²³ SST record. The dashed line indicates the 90.6% false alarm level.

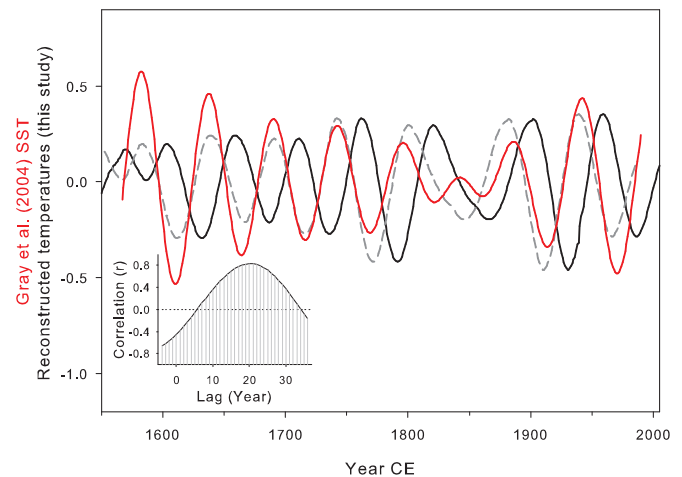


Figure 5 | Band-pass filtering at periods of the Atlantic Multidecadal Oscillation. Comparison of the 50–70 yr band-pass filtering results of the standardized PTP record of this study (black) with a proxy-based North Atlantic SST reconstruction²³ (red) for the past 500 yrs. The inset shows a lagged correlation curve. The highest correlation between the two series is achieved when the filtered PTP record is shifted by 20 years (dashed gray line).

band-pass filtered temperature record (Fig. 6) indicates that AMO intensity (or its influence on west Greenland's climate) was significantly higher during the last 2,000 years than prior to that. There is an intriguing period of particularly low variance from 2500–3500 BCE in the RABD_{660;670} record that potentially reflects an interval of very weak AMO variability. A 1,000 year period of suppressed AMO should be captured by other geological archives, and additional reconstructions are needed to validate this surprising result. Over the last 2,000 years, our record also indicates that variance in the AMO band was largest during the Mediaeval Climate Anomaly (MCA; ca. 950–1250 CE)²⁴ and reduced during the time interval associated with the Little Ice Age (LIA; 1250–1700 CE)²⁵. Suppressed variance in the AMO frequency band during the LIA relative to the MCA has also been suggested based on analyses of ice core proxy records from Greenland^{26,27}.

Recent model-based results suggest that the AMO is a 20th century phenomenon driven by anthropogenic aerosol emissions²⁸. However, our results indicate that the AMO has varied in intensity but has been a persistent mode of variability throughout the past 7,000 years. Aerosol forcing in the 20th century may have modulated the underlying AMO signal, but our results contradict the assertion that the AMO is purely anthropogenic.

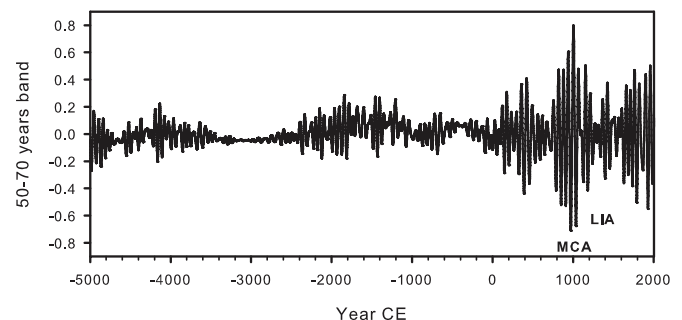


Figure 6 | Band-pass filtered record beginning -5000 years C.E. 50–70 year band-pass filtered data (corresponding to the period of the AMO) for the entire PTP-based reconstruction, from -5000 to 2005 CE.

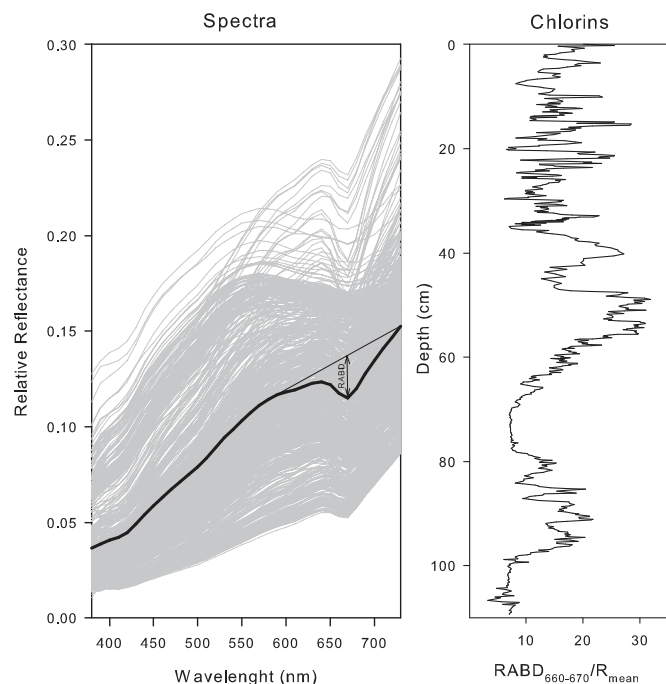


Figure 7 | Reflectance spectroscopy in the visible range for a sediment core from Braya Sø. (A) VIS-RS spectra from each 2 mm increment down core (length 120 cm). The bold line is the mean spectrum R_{mean} . (B) $RABD_{660-670}$ data (chlorin). $RABD_{660-670} = \{[(6 \cdot R_{590} + 7 \cdot R_{730})/13]/R_{min(660;670)}\}$, where R_{590} = reflectance at 590 nm, R_{730} = reflectance at 730 nm, $R_{min(660;670)}$ = minimum reflectance at 660 or 670 nm. Spectrum normalization and calculation of relative absorption band depths is fully described in ref. 7.

Discussion

There have been three principal approaches to proxy calibration. In the calibration-in-time (CIT) approach, proxy measurements spanning the monitoring interval are regressed against long-term climatic data. This approach has been used extensively in tree-ring research^{29,30} and has been applied in varved^{31–33} (annually laminated) and non-varved lakes^{11,15,34–36}, but requires excellent chronological control. For non-varved sediments, radionuclide dating (such as ^{210}Pb or ^{137}Cs) can be used, but this is often hampered by low concentrations of the species of interest, particularly in the Arctic. Without an extremely accurate chronology in the uppermost part of the sediment core, it is not possible to precisely compare proxy data to meteorological series. Furthermore, the accuracy and error of the age model influences the maximal temporal resolution and root square mean error of prediction (RSMEP) of the climate reconstruction. Thus it is not surprising that the majority of high-resolution and quantitative temperature reconstructions from Arctic lakes are based on varved sediments^{37–40}. Furthermore, for CIT to be successful, the top of the core must 1) be unaffected by non-climatic factors such as eutrophication or sediment slumping (turbidites), 2) have a sufficiently high sedimentation rate to provide a large enough sample set for statistically significant correlation, and 3) have an intact sediment-water interface to ensure the upper samples represent modern sedimentation³⁵. The CIT approach is further limited by the availability and quality of meteorological data. The Arctic generally has a very low density of meteorological stations with records usually covering fewer than 50 years. This makes the CIT approach particularly challenging and helps explain the scarcity of highly resolved and quantitative lake sediment temperature records from the Arctic⁴¹.

Another proxy calibration approach is the space-for-time (SFT) method, in which modern biological samples from lakes spanning a

spatial climatic gradient are used to develop a proxy calibration. This approach has been used to develop diatom and chironomid transfer functions in the Arctic^{42,43} and “global” TEX_{86} and branched tetraether temperature calibrations for lake sediments^{44–46}.

A third approach is to quantify the response of modern populations of organisms *in situ* to environmental parameters over one or more growth seasons. A calibration equation thus developed can then be applied to down-core sedimentary components. This approach has been successfully employed to develop lacustrine water temperature calibrations for alkenones, using the U_{37}^K index^{9,12}.

PTP calibration enables higher resolution paleoclimate reconstructions than are possible or practical using most sedimentological proxies of interest, due to the sampling limitations of those proxies. Another clear advantage of the PTP approach is that it can potentially be used in any region and type of environment. Unlike the CIT approach, PTP calibration does not depend on age model accuracy, which is often a limitation in non-varved lakes (the majority of lakes worldwide). Furthermore, for PTP calibration, the top of the sediment core need not be undisturbed or even intact. Another advantage is that the PTP correlations can be conducted using observed (*in situ*) data from the water column of the lake and the associated sediment core (as in this study), and is therefore possible even in the absence of a long local meteorological data set. Finally, PTP can substantially reduce the laboratory workload and costs associated with generating paleotemperature reconstructions. A statistically significant PTP calibration could be developed with as few as 50 correlation points (analyzed samples). Rapid scanning methods such as VIS-RS allow a meter of sediment to be analyzed at mm scale in under an hour. As demonstrated here, the PTP method can provide useful information, increasing both the length and temporal resolution of quantitative climate reconstructions.

Methods

Site. Lake Braya Sø ($66^\circ 59' 15''\text{N}$, $51^\circ 02' 0''\text{W}$, ca. 170 m a.s.l.) is located near Kangerlussuaq, West Greenland. It is a meromictic lake of 82 ha with a maximum depth of 24 m and a stable anoxic hypolimnion that favors preservation of pigments^{47,48}.

Alkenones. The details of lipid extraction are described in D’Andrea et al. (2011)⁹. Briefly, free lipids were extracted from freeze-dried and homogenized samples at 0.5 cm intervals and alkenones were quantified by gas-chromatography-flame-ionization-detection. The U_{37}^K -temperature calibration was established by combining *in situ* water temperature measurements made during two seasons of alkenone production in Braya Sø with previously published calibration data^{9,49}. $U_{37}^K = ([\text{C37:2}] - [\text{C37:4}]) / ([\text{C37:4}] + [\text{C37:3}] + [\text{C37:2}])$, where $[\text{C37:x}]$ = mass of the alkenone having 37 carbon atoms and x double bonds. U_{37}^K was originally defined in ref. 10.

VIS-RS. Because the sediment core (BS01-01) analyzed by D’Andrea et al. (2011)⁹ was consumed for alkenone analysis, the VIS-RS measurements were conducted on an overlapping core (BS03-01). The cores were easily stratigraphically aligned at mm-scale using laminations in the sediment (compared using high-resolution photographs from a Geotek Geoscan IV linescan). We measured VIS-RS (visible spectrum: 380–730 nm; spectral resolution: 10 nm) on the fresh unoxidized split sediment core at 2 mm intervals with a Spectrolino reflectance spectrometer (Gretag McBeth, Switzerland). The characteristic patterns of the reflectance spectra provide information on the composition and relative concentration of the sedimentary components. This method has been successfully used to measure organic compounds^{7,34,35} and lithogenic content^{50–52} in both marine and lake sediments. Here we use the parameter, Relative Absorption Band Depth at 660–760 nm ($RABD_{660-670}$)⁷, indicative of total early diagenetic chloropigments (chlorin), which have absorption peaks between 660–670 nm (I-band). $RABD_{660-670}$ was normalized by the mean spectrum reflectance ($RABD_{660-670}/R_{mean}$)⁷. Figure 7 shows the measured reflectance spectra of the sediment core of Braya Sø, the chlorin curve and how it is calculated.

Age model. The age model covering the last 7,000 years for Braya Sø is based on 6 AMS ^{14}C dates of bulk sediment, 3 of wood and 1 of a gastropod shell⁹. A reservoir effect correction of 360 years was applied to the ^{14}C dates prior to calibration⁹. The sediment core had an intact sediment-water interphase that was attributed the year 2005 CE of the coring⁹.

Numerical methods. The statistical basis of the PTP approach is a double calibration. First, we use the relation between the VIS-RS and alkenone data to transform the $RABD_{660-670}$ data into “inferred” alkenone U_{37}^K values. These values are then



transformed into temperatures using the U_{37}^K - temperature calibration. Because VIS-RS (2 mm) and alkenones (5–10 mm) were measured at a different resolution, the RABD_{660,670} data were re-sampled (linear interpolation) to match the U_{37}^K data resolution for this calibration.

We used the Pearson product-moment coefficient to determine the correlation between the RABD_{660,670} and U_{37}^K series. The P-values were corrected for trends and autocorrelation (P_c)⁵³.

To statistically evaluate the PTP calibration we used the split period calibration approach and calculated the reduction of error (RE) and coefficient of efficiency (CoE) values following the method of Cook et al. (1994)²⁹. The modern half of the samples was used for calibration and the older half for verification. We calculated the ten-fold cross-validated RMSEP using all depths to estimate the reconstruction error.

We used both an ordinary least squares regression (OLS) and Standard Major Axis regression (SMA) to transform the raw RABD_{660,670} series into “inferred U_{37}^K ” ($U_{37}^{K,i}$) values. These $U_{37}^{K,i}$ values were then transformed into temperatures with the U_{37}^K -temperature calibration ($T = 40.8 U_{37}^K + 31.8$, RMSEP: 1.3 °C) of D’Andrea et al. (2011)⁹. The final error of the reconstruction was calculated by summing (square root of the sum of the squares) the RMSEP (in °C) of the two calibrations.

The PTP VIS-RS temperature reconstruction presented here and the U_{37}^K reconstruction of D’Andrea et al. (2011)⁹ have non-regular temporal sampling intervals. Therefore, for the spectral analysis, we used the software REDFIT by Schulz and Mudelsee (2002)⁵⁴ allowing the input of unevenly spaced time series to estimate their red-noise spectrum and test if peaks in the spectrum of our temperature reconstructions are significant against a first-order autoregressive (AR1) model. False alarm levels were determined within the software package.

To determine whether the tree-ring based SST reconstruction²³ and our temperature reconstruction from Greenland share a common spectral phase in the domain of AMO, we calculated a Blackman-Harris 3-Term cross spectral analysis with the software SPECTRUM⁵⁵ (Fig. 5). The analysis was performed on the raw, unevenly spaced reconstruction series. A significant common spectral phase was identified in the range of 51–64 years.

We then band-pass filtered our reconstruction series and the SST data of Gray et al. (2004)²³ in the frequency band of AMO (50–70 years) using the Parks-McClellam algorithm. Because our reconstruction has non-regular temporal intervals, we linearly interpolated it to annual values before filtering it. Although data interpolation does introduce artifacts in the data series, their effect should be small in the low frequency band of interest. Means were removed before filtering. The spectral phase shift of 20 years between our band-pass filtered reconstruction and the band-pass filtered record by Gray et al. (2004)²³ was determined by cross-correlation analysis.

1. ACIA, Arctic Climate Impact Assessment. *Impacts of a Warming Arctic: Arctic Climate Impact Assessment* (Cambridge University Press, 2004).
2. CCSP, U.S. Climate Change Science Program. *Past Climate Variability And Change In The Arctic And At High Latitudes* (U.S. Geological Survey, 2009).
3. IPCC, Intergovernmental Panel on Climate Change. *Climate Change 2007 — The Physical Science Basis. Contribution Of Working Group I To The Fourth Assessment Report Of The IPCC* (Cambridge University Press, 2007).
4. Briffa, K. R., Jones, P. D., Schweingruber, F. H., Karlen, W. & Shiyatov, S. G. in *Climatic Variations And Forcing Mechanisms Of The Last 2000 Years* (ed. Jones, P. D., Bradley, R. S. & Jouzel, J.), NATO ASI Series 141, 9–41 (Springer, 1996).
5. Esper, J., Cook, E. R. & Schweingruber, F. H. Low-frequency signals in long tree-ring chronologies for reconstructing past temperature variability. *Science* **295**, 2250–2253 (2002).
6. Vinther, B. M. et al. Holocene thinning of the Greenland ice sheet. *Nature* **461**, 385–388 (2009).
7. Rein, B. & Sirocko, F. In-situ reflectance spectroscopy - analysing techniques for high-resolution pigment logging in sediment cores. *Int. J. Earth. Sci.* **91**, 950–954 (2002).
8. Elbert, J. et al. Systematic testing of in-situ reflectance spectroscopy (VIS-RS 380–730 nm) as a novel tool for biogeochemical analysis of lake sediments. *J. Paleolimnol.* (revised).
9. D’Andrea, W. J., Huang, Y., Fritz, S. C. & Anderson, N. J. Abrupt Holocene climate change as an important factor for human migration in West Greenland. *PNAS* (2011).
10. Brassell, S. C., Eglinton, G., Marlowe, I. T., Pflaumann, U. & Sarinthein, M. Molecular stratigraphy: A new tool for climatic assessment. *Nature* **320**, 129–133 (1986).
11. D’Andrea, W. J. et al. Mild Little Ice Age and unprecedented recent warmth in an 1800 year lake sediment record from Svalbard. *Geology* **40**, 1007–1010 (2012).
12. Castañeda, I. S. & Schouten, S. A review of molecular organic proxies for examining modern and ancient lacustrine environments. *Quaternary. Sci. Rev.* **30**, 2851–2891 (2011).
13. Toney, J. L. et al. Climatic and environmental controls on the occurrence and distributions of long chain alkenones in lakes of the interior United States. *Geochim. Cosmochim. Ac.* **74**, 1563–1578 (2010).
14. Willemse, N. W. & Törnqvist, T. E. Holocene century-scale temperature variability from West Greenland lake records. *Geology* **27**, 580–584 (1999).
15. McKay, N. P., Kaufman, D. S. & Michelutti, N. Biogenic silica concentration as a high-resolution, quantitative temperature proxy at Hallet Lake, south-central Alaska. *Geophys. Res. Lett.* **35**, (2008).
16. Hu, F. S. et al. Cyclic Variation and Solar Forcing of Holocene Climate in the Alaskan Subarctic. *Science* **26**, 1890–1893 (2003).
17. Kaplan, M. R., Wolfe, A. P. & Miller, G. H. Holocene Environmental Variability in Southern Greenland Inferred from Lake Sediments. *Quaternary. Res.* **58**, 149–159 (2002).
18. Michelutti, N. et al. Recent primary production increase in arctic lakes. *Geophys. Res. Lett.* **32**, (2005).
19. Douglas, S. V. & Smol, J. P. in *The Diatoms: Applications For The Environmental And Earth Sciences* (ed. Stoermer, E. F. & Smol, J. P.) 227–244 (Cambridge University Press, 1999).
20. Schlesinger, M. E. & Ramankutti, N. An oscillation in the global climate system of period 65–70 years. *Nature* **367**, 723–726 (1994).
21. Mann, M. E., Park, J. & Bradley, R. S. Global interdecadal and century-scale climate oscillations during the past five centuries. *Nature* **378**, 266–270 (1995).
22. Trenberth, K. E. & Shea, D. J. Atlantic hurricanes and natural variability in 2005. *Geophys. Res. Lett.* **33**, (2006).
23. Gray, S. T., Graumlich, L. J., Betancourt, J. L. & Pederson, G. T. A tree-ring based reconstruction of the Atlantic Multidecadal Oscillation since 1567 A.D. *Geophys. Res. Lett.* **31**, (2004).
24. Goosse, H. et al. The role of forcing and internal dynamics in explaining the “Medieval Climate Anomaly”. *Clim. Dyn.* (2012).
25. Grove, A. T. The “Little Ice Age” and its geomorphological consequences in Mediterranean Europe. *Climatic Change* **48**, 121–136 (2001).
26. Fischer, H. & Mieding, B. A 1,000-year ice core record of interannual to multidecadal variations in atmospheric circulation over the North Atlantic. *Clim. Dyn.* (2005).
27. Chylek, P. et al. Greenland ice core evidence for spatial and temporal variability of the Atlantic Multidecadal Oscillation. *Geophys. Res. Lett.* **39**, (2012).
28. Booth, B. B., Dunstone, N. J., Halloran, P. R., Andrews, T. & Bellouin, N. Aerosols implicated as a prime driver of twentieth-century North Atlantic climate variability. *Nature* (2012).
29. Cook, E. R., Briffa, K. R. & Jones, P. D. Spatial regression methods in dendroclimatology – a review and comparison of 2 techniques. *Int. J. Clim.* **14**, 379–402 (1994).
30. Esper, J., Frank, D. C., Wilson, R. J. S. & Briffa, K. R. Effect of scaling and regression on reconstructed temperature amplitude for the past millennium. *Geophys. Res. Lett.* **32**, (2005).
31. Trachsel, M., Eggenberger, U., Grosjean, M., Blass, A. & Sturm, M. 2008. Mineralogy-based quantitative precipitation and temperature reconstructions from annually laminated lake sediments (Swiss Alps) since AD 1580. *Geophys. Res. Lett.* **35**, (2008).
32. Francus, P., Bradley, R. S., Abbott, M. B., Patridge, W. & Keimig F. Paleoclimate studies of minerogenic sediments using annually resolved textural parameters. *Geophys. Res. Lett.* **29**, (2002).
33. Kalugin, I. et al. 800-yr-long records of annual air temperature and precipitation over southern Siberia inferred from Teletskoye Lake sediments. *Quaternary. Res.* **67**, 400–410 (2007).
34. von Gunten, L., Grosjean, M., Rein, B., Urrutia, R. & Appleby, P. G. A quantitative high-resolution summer temperature reconstruction based on sedimentary pigments from Laguna Aculeo, Central Chile, back to AD 850. *Holocene* **19**, 873–881 (2009).
35. von Gunten, L., Grosjean, M., Kamenik, C., Fujak, M. & Urrutia, R. Calibrating biogeochemical and physical climate proxies from non-varved lake sediments with meteorological data: methods and case studies. *J. Paleolimnol.* **47**, 583–600 (2012).
36. Koinig, K. A. et al. Environmental changes in an alpine lake (Gossenköllesee, Austria) over the last two centuries – the influence of air temperature on biological parameters. *J. Paleolimnol.* **28**, 147–160 (2002).
37. Cook, T. L., Bradley, R. S., Stoner, J. S. & Francus P. Five thousand years of sediment transfer in a high arctic watershed recorded in annually laminated sediments from Lower Murray Lake, Ellesmere Island, Nunavut, Canada. *J. Paleolimnol.* **41**, 77–94 (2009).
38. Huguen, K. A., Overpeck, J. T. & Anderson, R. F. Recent warming in a 500-year palaeotemperature record from varved sediments, Upper Soper Lake, Baffin Island, Canada. *Holocene* **10**, 9–19 (2000).
39. Thomas, E. K. & Briner, J. P. Climate of the past millennium inferred from varved proglacial lake sediments on northeast Baffin Island, Arctic Canada. *J. Paleolimnol.* **41**, 209–224 (2009).
40. Bird, B. W., Abbott, M. B., Finney, B. P. & Kutchko, B. A 2000 year varve-based climate record from the central Brooks Range, Alaska. *J. Paleolimnol.* **41**, 25–41 (2009).
41. Mann, M. E. et al. Proxy-based reconstructions of hemispheric and global surface temperature variations over the past two millennia. *PNAS* **105**, 13252–13257 (2008).
42. Larocque, I. & Bigler, C. Similarities and discrepancies between chironomid- and diatom-inferred temperature reconstructions through the Holocene at Lake 850, northern Sweden. *Quatern. Int.* **122**, 109–121 (2004).
43. Porinchu, D., Rolland, N. & Moser, K. Development of a chironomid-based air temperature inference model for the central Canadian Arctic. *J. Paleolimnol.* **41**, 349–368 (2009).
44. Powers, L. et al. Applicability and calibration of the TEX86 paleothermometer in lakes. *Org. Geochem.* **41**, 404–413 (2010).



45. Blaga, C. I. *et al.* Branched glycerol dialkyl glycerol tetraethers in lake sediments: Can they be used as temperature and pH proxies? *Org. Geochem.* **41**, 1225–1234 (2010).
46. Pearson, E. J., Juggins, S. & Farrimond, P. Distribution and significance of long-chain alkenones as salinity and temperature indicators in Spanish saline lake sediments. *Geochim. Cosmochim. Ac.* **72**, 4035–4046 (2008).
47. Carpenter, S. R., Elser, M. M. & Elser, J. J. Chlorophyll production, degradation, and sedimentation – implications for paleolimnology. *Limnol. Oceanogr.* **31**, 112–24 (1986).
48. Villanueva, J. & Hastings, D. W. A century-scale record of the preservation of chlorophyll and its transformation products in anoxic sediments. *Geochim. Cosmochim. Ac.* **64**, 2281–2294 (2000).
49. Zink, K. G., Leythaeuser, D., Melkonian, M. & Schwark, L. Temperature dependency of long-chain alkenone distributions in Recent to fossil limnic sediments in lake waters. *Geochim. Cosmochim. Ac.* **65**, 253–257 (2001).
50. Rein, B. *et al.* El Niño variability off Peru during the last 20,000 years. *Paleoceanography* **20**, (2005).
51. Trachsel, M., Grosjean, M., Schnyder, D., Kamenik, C. & Rein, B. Scanning reflectance spectroscopy (380–730 nm): a novel method for quantitative high-resolution climate reconstructions from minerogenic lake sediments. *J. Paleolimnol.* **44**, 979–994 (2010).
52. Elbert, J. *et al.* Quantitative high-resolution winter (JJA) precipitation reconstruction from varved sediments of Lago Plomo 47°S, Patagonian Andes, AD 1530–2001. *Holocene* (2011).
53. Trenberth, K. E. Some effects of finite sample size and persistence on meteorological statistics. *Mon. Weather Rev.* **112**, 2359–2368 (1984).
54. Schulz, M. & Mudelsee, M. REDFIT: Estimating red-noise spectra directly from unevenly spaced paleoclimatic time series. *Computers Geosci.* **28**, 421–426 (2002).
55. Schulz, M. & Stattegger, K. Spectral analysis of unevenly spaced paleoclimatic time series. *Computers Geosci.* **23**, 929–945 (1997).

Acknowledgements

We would like to thank J. Russell for producing the high-resolution photography of core BS03-01 and M. Grosjean for providing access to the reflectance spectrometer. We thank James Bendle and two anonymous reviewers for their positive and thoughtful comments, which have improved our manuscript.

This work was supported by the Swiss SNF (PBBEP2-126056 to LvG), US NSF (ARC-0402383 to YH and ARC-0851642 to WJD) and NOAA (NA09OAR4600215 and NA10OAR4310228 to RSB).

The new temperature reconstruction presented here is archived on the NOAA paleoclimate database at www.ncdc.noaa.gov/paleo/data.html.

Author contributions

WJD & YH collected the sediment core. LvG & WJD designed and performed research. LvG performed the statistical analyses. LvG, WJD, RSB & YH wrote and reviewed the manuscript.

Additional information

Competing financial interests: The authors declare no competing financial interests.

License: This work is licensed under a Creative Commons Attribution-NonCommercial-ShareAlike 3.0 Unported License. To view a copy of this license, visit <http://creativecommons.org/licenses/by-nc-sa/3.0/>

How to cite this article: von Gunten, L., D'Andrea, W.J., Bradley, R.S. & Huang, Y. Proxy-to-proxy calibration: Increasing the temporal resolution of quantitative climate reconstructions. *Sci. Rep.* **2**, 609; DOI:10.1038/srep00609 (2012).